Article

pubs.acs.org/Biomac

# Self-Assembled Stimuli-Responsive Polyrotaxane Core−Shell Particles

Blaise L. Tardy, Henk H. Dam, Marloes M. J. Kamphuis, Joseph J. Richardson, and Frank Caruso*

Department of Chemical and Biomolecular Engineering, The University of Melbourne, Victoria 3010, Australia

Supporting Information

**ABSTRACT:** Thermodynamically assembled core−shell nanocarriers are potential candidates for drug delivery applications due to their submicrometer size and the ability to load drugs into their hydrophobic core. Herein, we describe the formation of core−shell particles that consist of noncovalent polymers, that is, polyrotaxanes (PRXs), that form an α-cyclodextrin (αCD) core surrounded by a corona of low-fouling poly(ethylene glycol) (PEG). The PRX core−shell particles are able to sequester small organic molecules, such as pyrene and calcein, releasing these small molecules during degradation. The small, cellular peptide, glutathione, was used to degrade the particles through the reductive cleavage of disulfide bonds that stabilize the individual PRX polymers. Cleavage of a single bond allows for the degradation of the supramolecular-polymer, making these PRX core−shell particles highly responsive. Furthermore, these particles demonstrate negligible cytotoxicity in mammalian cells, making them promising carriers for future drug delivery research.

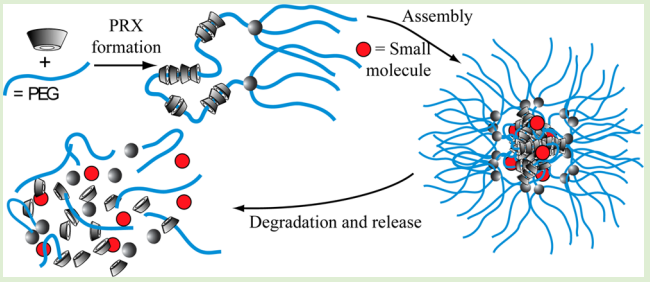


## INTRODUCTION

The design and development of efficient nanocarriers for targeted cargo release has attracted significant attention for biomedical applications because they offer the possibility of increasing specific therapeutic effects while decreasing nonspecific side effects.[1−4] Carrier systems based on self-assembled polymeric core−shell particles are particularly promising drug delivery vehicles, as they are often composed of block-polymers that allow the particles to partition into a hydrophobic drug-loaded core and a hydrophilic stealth corona. Although particles based on natural building blocks can improve the biodistribution of therapeutics,[4] carriers composed of synthetic macromolecular building blocks offer a number of benefits.[2] Specific characteristics of synthetic macromolecules and polymers can be tuned for control over biofouling, size, and bioresponsiveness.[5,6] For thermodynamically stabilized particles, these properties are largely determined by the physical and chemical properties of the chosen macromolecular building blocks.

Polyrotaxanes (PRX), composed of poly(ethylene glycol) (PEG) threaded by α-cyclodextrins (αCDs) in a reversible self-assembly process, are promising building blocks for core−shell nanocarriers due to their unique noncovalent structure.[7−9] One biomedically attractive property of PRXs is the ability to disassemble[10−12] into low-toxicity components (e.g., αCDs and PEG).[13,14] Furthermore, the self-assembly process of PRXs allows for straightforward control over their structural properties, such as size, which can be tuned by adjusting the PEG length; and rigidity, which can be varied by adjusting the degree of αCD threading.[15,16] Furthermore, threaded αCDs can be readily postmodified to allow for the introduction of additional functionality such as charged groups,[10] therapeutics, or targeting ligands.[17,18] The latter has been used to enhance multivalent interactions in biological systems because the rotational and lateral mobility of αCDs along the PEG chains accounts for the efficiency of binding to receptors. This αCD mobility also promotes stabilization in core−shell particles due to the cyclodextrin−cyclodextrin interactions in the particle core.[17,18]

We previously reported the preparation of degradable polyrotaxane microcapsules through layer-by-layer assembly[10] and polymer grafting,[23] in each case using particle templates for the formation of the films. Herein, we sought to assemble degradable polyrotaxane building blocks via template-free self-assembly for drug loading and release. Although self-assembled core−shell particles from ABA polyrotaxane polymers for the selective encapsulation and release of hydrophobic therapeutics have been reported,[19−22] these particles are not degradable, thereby potentially limiting their application in biological and biomedical studies. In the current study we demonstrate the one-step formation of degradable, self-assembled core−shell particles composed of triblock polyrotaxanes (Scheme 1). The ABA triblock architecture was synthesized via a modular approach using alkyne−azide click chemistry,[23,24] allowing for additional modifications using the same chemistry. These PRX core−shell particles are degradable under mild reducing

Received: August 22, 2013
Revised: October 21, 2013
Published: December 13, 2013

  

**Scheme 1. Preparation of PRX 6 Core-Shell Particles**[a]

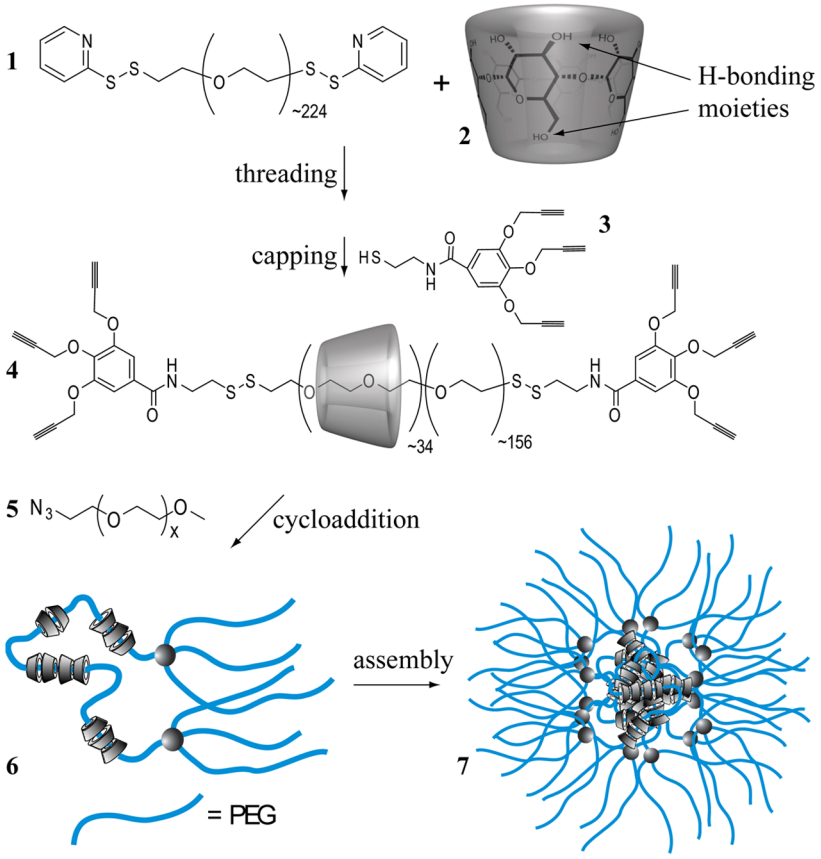


[a]PEG **1** is self-assembled with αCDs to form PPRXs. This is followed by end-capping of the PEG chains with **3**, giving PRX **4**. PRX **4** is modified with azide functionalized PEG **5** using click chemistry. Triblock PRX **6** self-assembles in water into core-shell particles **7** via intra- and intermolecular H-bonding between threaded αCDs.

conditions through the cleavage of the disulfide bonds that link the blocking groups to the PEG backbone. This process is anticipated to be highly sensitive, as one cleavage event allows a high molecular weight PRX to degrade into its initial, "preassembly" (pristine) components. This sensitivity is demonstrated by the degradation of stable core−shell particles under physiologically relevant conditions.[25] Furthermore, the negligible cytotoxicity in cells, submicrometer size, use of low-fouling PEG chains in the blocking groups, and capacity for loading and releasing small hydrophobic molecules suggest that these particles could find application in drug delivery.

## EXPERIMENTAL SECTION

**Materials.** High-purity water (Milli-Q (MQ)) with a resistivity of >18 MΩ·cm was obtained from an in-line Millipore RiOs/Origin water purification system. The pH of solutions was measured with a Mettler-Toledo MP220 pH meter. Silicon wafers were obtained from MMRC Pty (Melbourne, Australia). Glutathione (GSH), copper sulfate, sodium-L-ascorbate, phosphate buffer saline (PBS), calcein, α-cyclodextrin, dimethylformamide (DMF), dimethylsulfoxide (DMSO), and dithiothreitol (DTT) were obtained from Sigma-Aldrich, *N*,*N*′-disuccinimidyl carbonate (diNHS) from Fluka, homobifunctionalized *o*-pyridyldisulfide-poly(ethylene glycol) (OPSS-PEG-OPSS), $M_w$ 10 kDa, from Creative PEGWorks, and PEG-azide ($M_w$ 5 kDa) was obtained from JenKem Technology U.S.A. Dulbecco's Modified Eagle Medium (DMEM) and Fetal Bovine Serum (FBS) were purchased from GIBCO. MTT was purchased from Sigma-Aldrich. All chemicals were used as received. The capping group **3** was synthesized according to a procedure previously reported.[23] NMR spectra were recorded using a 400 MHz Varian INOVA system at 25 °C. The spin−lattice relaxation time ($T_1$) was determined at 24 °C via a conventional inversion recovery pulse sequence, 90°−*t*−180°, under deuterium lock mode. Spectra were referenced to residual proton resonances of the deuterated solvent. Chemical shifts are reported as parts per million (ppm) downfield from the signal originating from TMS (trimethylsilyl). The fluorescence intensity of released calcein (excitation 480 nm, emission 580 nm) was measured with a Horiba Fluorolog spectrophotometer using a 200 μL quartz cuvette.

**Polyrotaxane 4.** OPSS-PEG-OPSS, 10 kDa, **1** (0.089 g, 0.026 mmol) was dissolved in 0.5 mL of $H_2O$. The PEG solution was added to a concentrated solution of αCD **2** (1.94 g, 1.99 mmol) in 18 mL of $H_2O$. Within several minutes a white precipitate was formed, indicating the formation of pseudopolyrotaxane (PPRX) assemblies. The suspension was ultrasonicated for 1.5 h, followed by shaking overnight at 24 °C. The precipitate was collected by centrifugation at 5000 *g* for 5 min and the supernatant was decanted. Freeze-drying gave 0.960 g of PPRX as a white powder that contained a fraction of nonthreaded αCD. Capping group **3** (0.010 g, 0.029 mmol) was mixed with 0.150 g PPRX in a 2.0 mL vial. DMF (0.15 mL) was then added, upon which the mixture was vortexed until a thick yellow suspension was formed (within minutes). The suspension was ultrasonicated for 1.5 h, after which 1.5 mL of acetone was added and the precipitate was washed with 5 × 1.5 mL of acetone (until the washing was colorless) and with 4 × 1.5 mL of $H_2O$. The crude product was dissolved in 2.0 mL of DMSO and precipitated with 2.0 mL of $H_2O$. This cycle was repeated five times to ensure that all nonthreaded αCDs and PEG were removed. The precipitate was freeze-dried to give 0.082 g PRX **4** as a white powder. $^1$H NMR (400 MHz, DMSO-$d_6$): 7.30 (s, 4H, Ph), 5.66 (s, broad, 34 × 6H, OH-2 of αCD), 5.50 (s, broad, 34 × 6H, OH-3), 4.80 (s, broad, 34 × 6H, H-1 of αCD), 4.43 (s, broad, 34 × 6H,


dx.doi.org/10.1021/bm401244a | *Biomacromolecules* 2014, 15, 53−59

OH-6 of αCD), 3.74−3.27 (m, broad, 34 × 36H, H-3, H-4, H-5, and H-6a,b, of αCD), 3.51 (s, 896H, -$OCH_2CH_2O$- of PEG). The number of threaded αCDs per PEG chain was determined to be 34 by integration of the CH-1 signal at 4.80 ppm and the $CH_2CH_2$ (PEG) protons at 3.51 ppm (see Supporting Information). $^{13}C$ NMR (DMSO-$d_6$): δ 102.0 (C-1 αCD), 82.1 (C-4 αCD), 73.4 (C-3 αCD), 72.1 (C-5 αCD), 71.6 (C-2 αCD), 69.8 ($CH_2CH_2$−O), 69.4 (broad, complexed $CH_2CH_2$−O),[26] 59.6 (C-6 αCD). IR: ν ($cm^{-1}$) = 3431 (s, broad; O−H αCD), 2917 (s; −$CH_2$ PEG), 2255 (s, broad; C≡C), 1647 (s, HNC═O).

**Polyrotaxane 6.** $CuSO_4$ ($8.4 \times 10^{-4}$ g) dissolved in 10 μL of MQ water was mixed with $3.6 \times 10^{-3}$ g chelator (a Cu-chelator was used to stabilize the Cu (I) and (II) species, see ref 24) dissolved in 40 μL of DMSO, giving a blue solution, indicative of the presence of the chelator−Cu(II) complex. A solution of $1.1 \times 10^{-3}$ g sodium ascorbate in 5 μL MQ water was added, giving a green solution, indicative of the presence of the chelator−Cu(I) complex. To this mixture, a solution of PRX **4** ($20 \times 10^{-3}$ g) and PEG-azide 5 kDa **5** ($32 \times 10^{-3}$ g) in 200 μL DMSO was added. The resulting mixture was shaken at 24 °C for 18 h at 1500 *g*, upon which it was diluted with 500 mL MQ water and dialyzed (12.4 kDa MWCO membrane) over 2 × 1.8 L MQ water (pH 9) for 2 × 3 h and 2 × 1.8 L MQ water (pH 5) for 2 × 24 h. The dialyzed solution was freeze-dried, giving $3.4 \times 10^{-2}$ g PRX **6** as a white compound. $^1H$ NMR (400 MHz, $D_2O$): 5.07 (d, 34 × 6H, *J* = 3.3 Hz, H-1 of αCD), 4.01 (t, 34 × 6H, *J* = 9.3 Hz, H-3 of αCD), 3.94−3.82 (m, 34 × 18H, H-6a,b and H-5 of αCD), 3.72 (s, 3636H, -$OCH_2CH_2O$- of PEG), 3.72−3.58 (m, 34 × 12H, H-4 and H-2 of αCD). IR: ν ($cm^{-1}$) = 3367 (s, broad; O−H αCD), 2882 (s; −$CH_2$ PEG), 1647 (s, broad; HNC═O). For MALDI-TOF and NMR spectra, see Supporting Information.

**Atomic Force Microscopy (AFM).** AFM images were obtained with an MFP-3D Asylum Research instrument. Typical scans were conducted in AC mode with ultrasharp SiN gold-coated cantilevers (NT-MDT). Samples were prepared by dropping 1 μL of a solution of PRX **6** on a freshly cleaned silicon wafer slide followed by drying at 24 °C.

**Transmission Electron Microscopy (TEM).** TEM images were obtained with a FEI Tecnai F30 transmission electron microscope operated at 200 kV. Samples were prepared by dropping 1 μL of a solution of PRX **6** on carbon-coated 300 mesh copper grids (ProSciTech, Australia) followed by drying at 24 °C.

**Determination of the Critical Aggregation Concentration (CAC).** A 1 M solution of pyrene in acetone was diluted to $6 \times 10^{-6}$ M in water. Subsequently, this solution was used to determine the CAC by dissolving PRX with a concentration ranging from 10 to $10^{-7}$ g $L^{-1}$. Pyrene emission was measured at 383 nm (excitation at 338 nm, 2 nm bandpass). The signal was integrated over 1 s. Fluorescence spectrophotometry experiments were carried out on a Fluorolog-3 Model FL3−22 spectrofluorometer.

**Dynamic Light Scattering (DLS).** DLS measurements were performed using 0.1 to 0.5 mg $mL^{-1}$ solutions of core−shell particles in a Nano ZS model ZEN3600 with a scattering angle of 173°.

**Preparation of PRX 6 Core−Shell Particles.** General procedure: PRX **6** (0.4 mg) was dissolved in 0.4 mL of MQ water or in a 0.4 mL solution of 100 mM calcein and 200 mM phosphoric acid at pH 7.4 and left to equilibrate for ≥18 h at 24 °C. Subsequently, the mixture was sonicated for 25 min at 24 °C.

Preparation of PRX **6** core−shell particles followed by extrusion: PRX **6** (0.5 mg) was dissolved in 0.2 mL of DMSO and left to evaporate in a 10 mL flask on a rotary evaporator under reduced pressure. A total of 1 mL of MQ water was then poured onto the film to make a 0.5 g $L^{-1}$ solution. The solution was then extruded using a polycarbonate membrane with a pore size of 200 nm.

**Degradation of PRX 6 Core−Shell Particles.** Calcein is a fluorescent dye with excitation and emission wavelengths of 495 and 515 nm, respectively. Upon self-quenching, calcein turns red. Calcein is known to self-quench at concentrations as low as ∼70 mM.[27] Calcein was used as an indicator for the presence and degradation of the core−shell particles by encapsulating it in the hydrophobic core. Prior to all degradation experiments, the core−shell particles were dialyzed using a regenerated cellulose membrane of MWCO 12.3 kDa for 72 h at 24 °C over 5 × 2 L 4 mM phosphoric acid buffered at pH 7.4. The presence of a strong red color in the dialysis bag suggested that the concentration of calcein inside the core−shell particles was above its quenching concentration (a dilute solution is yellowish). The samples were then diluted to 0.05 mg $mL^{-1}$ in 4 mM phosphoric acid solution (pH 7.4) and were analyzed with a fluorescence spectrophotometer before and after initiation of the degradation experiments by the addition of either GSH or DTT to a final concentration of 5 mM.

The degradation of PRX **6** core−shell particles was also followed by measuring the intensity of the scattered light at an angle of 173°. The light scattering of a 2.5 mg $mL^{-1}$ solution of PRX **6** containing 5 mM GSH was measured over time. The measurements started immediately after preparation of the solution. The blank consisted of the same concentration of PRX **6** core−shell particles in MQ water.

**Cell Viability Assay.** Early passage HeLa cells were seeded in a 96-well plate at a density of $5 \times 10^3$ cells × $well^{-1}$ and cultured in DMEM supplemented with 10% FBS and 2 mM GlutaMAX at 37 °C in 5% $CO_2$. The cells were exposed to varied concentrations of the PRX **6** core−shell particles in a total volume of 200 μL for 48 h. After aspirating the supernatant of each well and washing with PBS, 180 μL of the supplemented DMEM and 20 μL of MTT solution (5 mg $mL^{-1}$ in PBS) were added to the wells. Plates were further incubated at 37 °C in 5% $CO_2$ for 2 h. After the addition of 200 μL of solubilization mixture (0.04 N HCl in isopropanol), the absorbance at 560 nm (blue formazan) was measured with a plate reader (Multiskan Ascent, Thermo Scientific). The absorbance of control wells without MTT was subtracted. All experiments were performed in quadruplicate and the relative cell viability was normalized relative to the untreated control cells.

## RESULTS AND DISCUSSION

### Formation and Characterization of the PRX Assembly.

PRX **4** was synthesized by starting with commercially available bis(*o*-pyridyldisulfide) poly(ethylene glycol) (OPSS-PEG-OPSS) **1** of $M_w$ 10 kDa containing activated thiol groups at both ends (Scheme 1). The OPSS-PEG-OPSS was threaded with αCDs following the method reported by Harada and Kamachi,[28] in which the PEG is mixed with a concentrated solution of αCD at 24 °C, giving PPRXs as a white precipitate. The PPRXs are soluble in DMF or DMSO; however, solubilization is accompanied by dethreading of the αCDs[29] because αCD-PEG inclusion is largely based on hydrophobic interactions and thus is most efficient in water. PRX formation was, therefore, performed in suspension using a sufficiently fast capping reaction to avoid significant dethreading. The formation of PRX **4** was performed according to a procedure developed previously.[23] The presence of the disulfide groups allows dethreading of these PRXs under reducing conditions. Inter- and intramolecular hydrogen bonding (H-bonding) between threaded αCDs in PRXs decreases their solubility in water, and above a certain threading degree, PRXs become insoluble in water, which allows them to be separated from free αCDs and unthreaded PEG chains. In the $^1H$ NMR spectrum of **4**, a characteristic broadening of αCD proton peaks was observed, owing to its reduced mobility in the threaded state.[30] From integration of the areas of the C*H*-1 signal at 4.80 ppm and the $CH_2CH_2$ protons of the PEG chain at 3.50 ppm, the average number of threaded αCDs was determined to be on average 34 per PEG chain. The length of two PEG monomeric units corresponds to the cavity size of one αCD.[31] PEG of 10 kDa has ∼224 monomeric units, so the maximum number of αCDs that can be threaded is therefore ∼112. With 30% threading, the structure of PRX **4** is flexible, which allows the threaded αCDs to rotate and slide over the PEG backbone. The


dx.doi.org/10.1021/bm401244a | *Biomacromolecules* 2014, 15, 53−59

$^1$H spin−lattice relaxation time ($T_1$) of the C*H*-1 protons in threaded αCDs is 1.110 ± 0.007 s, which is similar to that of the C*H*-1 protons of free αCD (1.090 ± 0.009 s). This indicates that the threaded αCDs in PRX **4** have significant mobility since the $T_1$ of a PRX with 82% threading degree, in which the αCDs have a decreased mobility, is 1.500 ± 0.043 s.[23] The characteristic broad signals due to the threaded αCDs disappeared when 5 mM GSH was added and the OH-2 and OH-3 signals from αCD shifted to higher field, 5.66 to 5.55 ppm and 5.50 to 5.46 ppm, respectively, confirming disassembly of PRX **4** by reductive cleavage of the disulfide bonds. To obtain a water-soluble PRX, PRX **4** was modified by clicking azide functionalized PEG moieties ($M_w$ 5 kDa) **5**, using the Cu(I)-catalyzed alkyne−azide click reaction, onto the capping groups giving PRX **6**. We have used this type of click chemistry previously for the end-functionalization of rigid PRXs that were assembled on a particle surface.[23] The main reasons for employing alkyne−azide click chemistry is that this reaction proceeds under mild conditions and yields a highly stable triazole ring, making it attractive for the encapsulation of therapeutics.[32] We anticipate that the high specificity of this reaction opens possibilities to create PRX core−shell particles with a broad range of functional groups at their surface, such as antibodies[24] that are relevant for the active targeting of drug carriers.

The previously mentioned inter- and intramolecular H-bonding between threaded αCDs are fundamental for the formation of core−shell particles (Scheme 1).[33−35] Threaded CDs preferably hydrogen bond with each other, excluding water in the process. This reduction in water content makes the core inherently more hydrophobic. It is likely that the flexible nature of PRX **6** will aid in the stability of the formed core−shell particles by allowing threaded αCDs to slide and rotate over the PEG backbone and adopt thermodynamically favorable positions within the hydrophobic interior, thus resulting in more efficient H-bonding between PRXs. It was found that a triblock polymer analog of PRX **6** that contained PEG moieties of $M_w$ 2 kDa instead of 5 kDa yielded particles that formed large aggregates. These aggregates precipitated from a clear DMSO solution in water after several minutes. Core−shell particles formed from PRX **6** are, however, stable for more than 3 months (data obtained from DLS are similar within this time frame), illustrating the importance of the hydrophobic to hydrophilic ratio in this system. From $M_w$ analysis, 30 kDa of PEG as the hydrophilic group (6 × 5 kDa) is necessary to suspend, in a self-assembled structure, the hydrophobic group consisting of 34 cyclodextrins ($M_w$ of 33320). Previous work has shown that, in the case of miktoarm-containing structures, the volume fraction of hydrophilic to hydrophobic groups, rather than the length or number of miktoarms, is the determining parameter in the assembly formation.[36]

After dissolving PRX **6** in MQ water a polydisperse system is formed (Figure 1a). The size distribution of the core−shell particles composed of PRX **6** can be narrowed to 285 ± 55 nm by using either extrusion or sonication for 30 min in the preparation procedure (Figure 1b,c). Extrusion using membranes with pore sizes of 50, 100, or 400 nm did not result in a significant improvement in size distribution of the core−shell particles, suggesting that this particular process might not be particularly relevant to polyrotaxane-based triblock architectures.

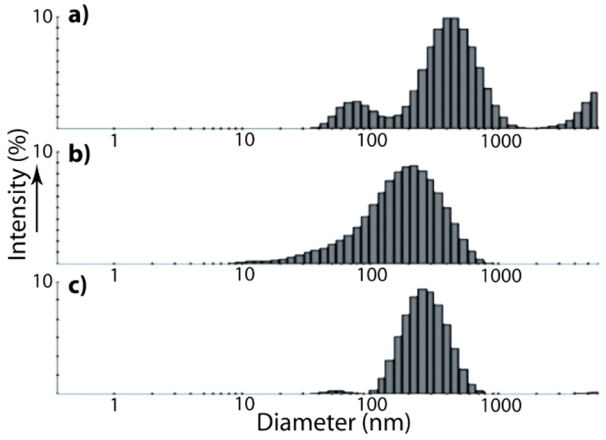


**Figure 1.** DLS measurements of PRX **6**: (a) after solubilizing in water, and (b) extrusion using a 200 nm pore size polycarbonate membrane, or (c) sonication for 30 min.

Pyrene was used as a fluorescence probe to determine the CAC of the core−shell particles.[37] A large shift in the intensity ratio, $I_1$ (372 nm) over $I_3$ (383 nm), was observed when increasing the concentration of PRX **6** in MQ, which is indicative of incorporation of pyrene in a hydrophobic core (Figure 2). The CAC was determined to be 2.5 × $10^{-4}$ mM,

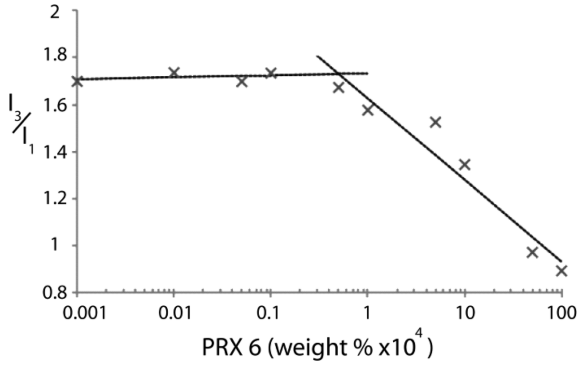


**Figure 2.** Determination of the CAC of PRX **6** core−shell particles by fluorescence spectroscopy using pyrene as a fluorescence probe. $I_3$ corresponds to pyrene emission at 383 nm and $I_1$ to pyrene emission at 372 nm.

which is an order of magnitude higher compared with other PRX-based core−shell particles[12,14] and of the same order that is found for other core−shell particles based on conventional triblock copolymers.[35]

AFM imaging of air-dried PRX **6** core−shell particles formed via extrusion gave a diameter of approximately 100 nm and a thickness of 5 nm (Figure 3). Compared to the DLS data, AFM shows smaller particles, which are most likely the result of the adsorption of the PEG moieties on the $SiO_2$ surface via hydrogen bonding[38] followed by dehydration of the core−shell particles due to the drying of the samples. The size of the core−shell particles, as observed in the AFM images, is in accordance with the size of the (air-dried) core−shell particles that were observed by TEM (Figure 4).

**Degradation of the PRX Core−Shell Particles.** The degradation of PRX **6** core−shell particles is initiated by cleavage of the disulfide bonds, leading to the removal of the blocking groups on which the PEG corona is attached. The hydrophobic core degrades further as the αCDs dethread from


dx.doi.org/10.1021/bm401244a | *Biomacromolecules* 2014, 15, 53−59

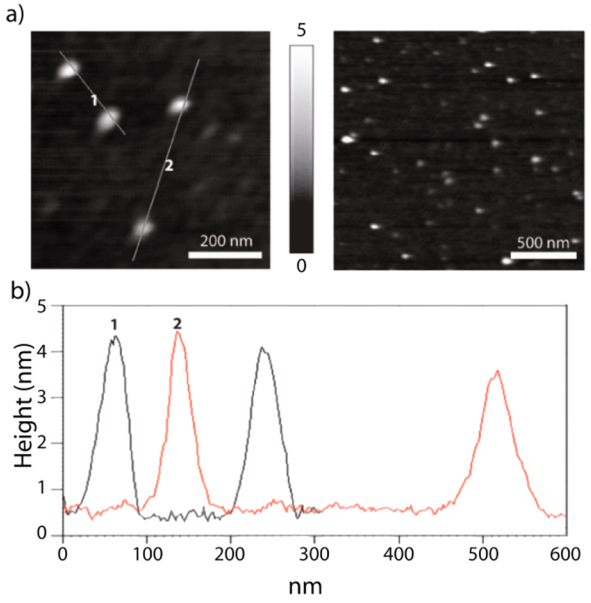


**Figure 3.** AFM images and cross-section profile of air-dried PRX **6** core–shell particles.

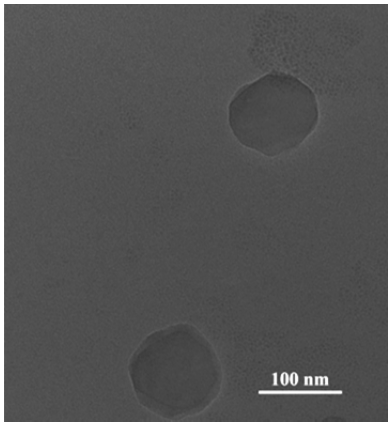


**Figure 4.** TEM images of PRX **6** core–shell particles formed and extruded through a 200 nm polycarbonate membrane.

the PPRXs. The kinetics of dethreading are related to the extent of H-bonding between the PPRXs. The pyrene assay suggests the presence of a rather dense hydrophobic core. Therefore, degradation of the core was followed by measuring the scattered light intensity (Figure 5). A decrease in the light scattering intensity after exposure of the core–shell particles to a concentration of 5 mM GSH is indicative of degradation. After the first 60 min of degradation, the signal dropped to about 35% of the original value, after which the kinetics slowed. This is likely the result of GSH being oxidized by $O_2$ over the course of the experiment. A negligible difference in scattered light was observed over time in the absence of GSH.

Degradation of the PRX **6** core–shell particles was also studied using calcein as a probe. Calcein was incorporated in the core at concentrations high enough to induce self-quenching. Upon degradation (with GSH or DTT), calcein is released and diluted, resulting in a fluorescence signal increase at 515 nm (Figure 6). Generally, calcein leakage from micelles is minimal with no major effect upon exposure to a surfactant. In contrast calcein leakage out of polymersomes over time is considerable and follows a burst release profile upon

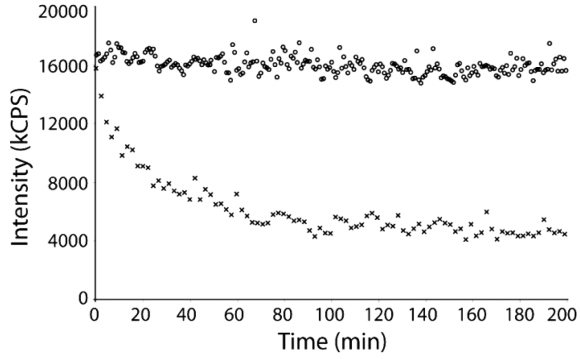


**Figure 5.** Light scattering intensity (173°) of a solution of PRX **6** plotted against time. Upper points correspond to a solution of 2.5 mg $mL^{-1}$ PRX **6**. The lower points correspond to the signal observed directly after the addition of GSH to a final concentration of 5 mM to a solution of 2.5 mg $mL^{-1}$ PRX **6**.

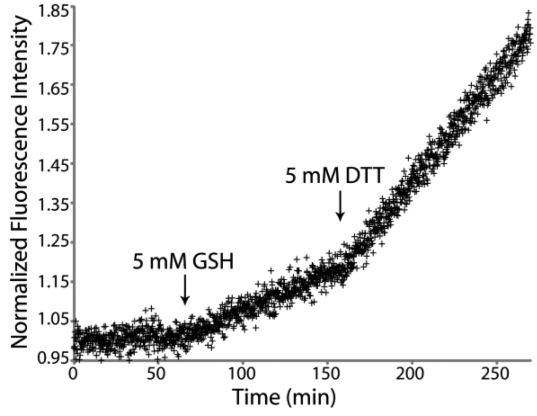


**Figure 6.** Degradation of PRX **6**-based core–shell particles observed by measuring the fluorescence of released calcein at 515 mm from calcein-loaded core–shell particles. Arrows indicate time of addition of the reducing agents GSH or DTT.

degradation (i.e., in the presence of surfactants).[38] The PRX core–shell particles were formed in a solution containing 0.1 M calcein. After formation of the core–shell particles, the excess calcein was removed by dialysis for 2 weeks with replenishing the dialysis solution at regular time intervals. The PRX **6** solution showed a red color, indicating the presence of sequestered calcein. Release of calcein from PRX **6** core–shell particles in the absence of reducing agent was studied by dialyzing 1 mL of a 0.1% solution of calcein loaded core–shell particles in 50 mL of dialysis solution using a 7 kDa MWCO membrane and monitoring the fluorescence change of the dialysis solution. There was no significant change in the fluorescence over a period of 1 month. The addition of the surfactant Triton-X at a final concentration of 10 mg $mL^{-1}$ did not affect the calcein release. Both observations suggest that PRX **6** forms core–shell particles under the conditions used.[39]

Upon addition of GSH, a linear increase in fluorescence intensity was observed. After 200 min, the stronger reducing agent DTT was added at a total concentration of 5 mM. This resulted in an increase in the degradation kinetics, suggesting cleavage of the disulfide bonds is rate limiting. The difference in kinetics might also be due to the fact that when disulfide cleavage occurs with both of these reducing agents, an intermediate is formed where the chain end is replaced by the reducing agent. GSH would form a semiblocking group,


dx.doi.org/10.1021/bm401244a | *Biomacromolecules* 2014, 15, 53–59

slowing the release of cyclodextrin from polyrotaxanes, while DTT would not inhibit the dethreading process.

To examine the toxicity of the PRX **6** core−shell particles a cell viability study was performed. This study showed that the PRX **6** core−shell particles show no significant toxicity to HeLa cells up to a concentration of 0.062 mg $mL^{-1}$ (Figure 7), after

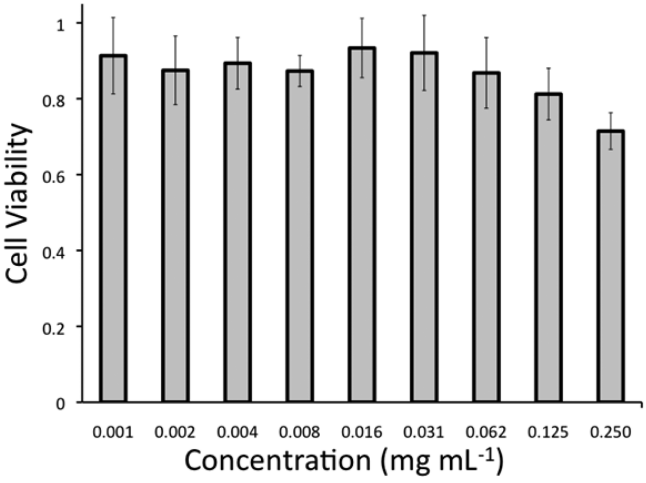


**Figure 7.** Cell viability assay of the PRX **6** core−shell particles at different final concentrations.

which the toxicity increased gradually to give a cell viability of about 70% at 0.25 mg $mL^{-1}$. This further highlights the potential use of these particles for drug delivery applications.

## CONCLUSIONS

We have reported the synthesis of degradable PRXs and the fabrication of degradable core−shell particles using PRX building blocks. The presence of disulfide bonds between the blocking groups and the PEG chains in the PRXs allows triggered degradation under simulated intracellular reducing conditions. The degradation kinetics are determined by a combination of disulfide cleavage and dethreading of the CDs, suggesting it is possible to tune the system by modifying the PEG chain length, the degree of threaded CDs, or the side polymer component attached to the blocking group. The unique composition of PRX core−shell particles and the resulting degradation properties opens up new possibilities for the delivery of small therapeutics, especially when considering the potential control over the degradation kinetics. CDs can be readily modified and conjugated with functional groups, drugs, and ligands, which should make it possible to obtain highly sensitive PRX core−shell particles with a wide variety of biomedically relevant properties.

## ASSOCIATED CONTENT

### Supporting Information

MALDI-TOF and NMR data for PRX **6** and PRX **4**. This material is available free of charge via the Internet at http://pubs.acs.org.

## AUTHOR INFORMATION

### Corresponding Author

*E-mail: fcaruso@unimelb.edu.au.

### Notes

The authors declare no competing financial interest.

## ACKNOWLEDGMENTS

F.C. acknowledges funding from the Australian Research Council under the Australian Laureate Fellowship Scheme (FL120100030, F.C.).

## REFERENCES

(1) Petros, R. A.; DeSimone, J. M. *Nat. Rev. Drug Discovery* **2010**, *9*, 615−627.
(2) Peer, D.; Karp, J. M.; Hong, S.; Farokhzad, O. C.; Margalit, R.; Langer, R. *Nat. Nanotechnol.* **2007**, *2*, 751−760.
(3) Li, M.-H.; Keller, P. *Soft Matter* **2009**, *5*, 927−937.
(4) (a) Meng, F.; Zhong, Z.; Feijen, Y. *Biomacromolecules* **2009**, *10*, 197−209. (b) Cerritelli, S.; Velluto, D.; Hubbell, J. A. *Biomacromolecules* **2007**, *8*, 1966−1972.
(5) Renggli, K.; Baumann, P.; Langowska, K.; Onaca, O.; Bruns, N.; Meier, W. *Adv. Funct. Mater.* **2011**, *21*, 1241−1259.
(6) LoPresti, C.; Lomas, H.; Massignani, M.; Smart, T.; Battaglia, G. *J. Mater. Chem.* **2009**, *19*, 3576−3590.
(7) Harada, A.; Li, J.; Kamachi, M. *Nature* **1993**, *364*, 516−518.
(8) Harada, A.; Hashidzume, A.; Yamaguchi, H.; Takashima, Y. *Chem. Rev.* **2009**, *109*, 5974−6023.
(9) Wenz, G.; Han, B. H.; Mueller, A. *Chem. Rev.* **2006**, *106*, 782−817.
(10) Dam, H. H.; Caruso, F. *Langmuir* **2013**, *29*, 7203−7208.
(11) Dam, H. H.; Caruso, F. *Adv. Mater.* **2011**, *23*, 3026−3029.
(12) Ooya, T.; Choi, H. S.; Yamashita, A.; Yui, N.; Sugaya, Y.; Kano, A.; Maruyama, A.; Akita, H.; Ito, R.; Kogure, K.; Harashima, H. *J. Am. Chem. Soc.* **2006**, *12*, 3852−3853.
(13) Davis, M. E.; Brewster, M. E. *Nat. Rev. Drug Discovery* **2004**, *3*, 1023−1035.
(14) Wattendorf, U.; Kreft, O.; Textor, M.; Sukhorukov, G. B.; Merkle, H. P. *Biomacromolecules* **2008**, *9*, 100−108.
(15) Zhao, T.; Beckham, H. W *Macromolecules* **2003**, *36*, 9859−9865.
(16) Jarroux, N.; Guégan, P.; Cheradame, H.; Auvray, L. *J. Phys. Chem. B* **2005**, *109*, 23816−23822.
(17) Ooya, T.; Eguchi, M.; Nobuhiko, Y. *J. Am. Chem. Soc.* **2003**, *125*, 13016−13017.
(18) Ooya, T.; Utsunomiya, H.; Eguchi, M.; Nobuhiko, Y. *Bioconjugate Chem.* **2004**, *16*, 62−69.
(19) Zhang, X.; Ke, F.; Ye, L.; Liang, D.; Zhang, A.; Feng, Z. *Soft Matter* **2009**, *5*, 4797−4803.
(20) Yang, C.; Li, J. *J. Phys. Chem. B* **2009**, *113*, 682−690.
(21) Zhang, X.; Zhu, X.; Ke, F.; Ye, L.; Chen, E.; Zhang, A.; Feng, Z. *Polymer* **2009**, *50*, 4343−4351.
(22) Nagahama, K.; Ohmura, J.; Sakaue, H.; Ouchi, T.; Ohya, Y.; Nobuhiko, Y. *Chem. Lett.* **2010**, *39*, 250−251.
(23) Dam, H. H.; Caruso, F. *ACS Nano* **2012**, *6*, 4686−4693.
(24) Kamphuis, M. M. J.; Johnston, A. P. R.; Such, G. K.; Dam, H. H.; Evans, R. A.; Scott, A. M.; Nice, E. C.; Heath, J. K.; Caruso, F. *J. Am. Chem. Soc.* **2010**, *132*, 15881−15883.
(25) Hong, R.; Han, G.; Fernandez, J. M.; Kim, B.-J.; Forbes, N. S.; Rotello, V. M. *J. Am. Chem. Soc.* **2006**, *128*, 1078−1079.
(26) Harada, W.; Li, J.; Nakamitsu, T.; Kamachi, M. *J. Org. Chem.* **1993**, *58*, 7524−7528.
(27) Hiren Patel, H.; Tscheka, C.; Heerklotz, H. *Soft Matter* **2009**, *5*, 2849−2851.
(28) Harada, A.; Kamachi, M. *Macromolecules* **1990**, *23*, 2821−2823.
(29) Kalashnikov, P. A.; Sokolov, V. I.; Topchieva, I. N. *Russ. Chem. Bull., Int. Ed.* **2005**, *54*, 1973−1977.
(30) Zhao, T.; Beckham, H. W. *Macromolecules* **2003**, *36*, 9859−9865.
(31) Harada, A.; Li, J.; Kamachi, M.; Kitagawa, Y.; Katsube, Y. *Carbohydr. Res.* **1998**, *305*, 127−129.
(32) Meldal, M.; Tomoe, C. W. *Chem. Rev.* **2008**, *108*, 2952−3015.
(33) Nascimento, C. S., Jr.; Anconi, C. P. A.; Dos Santos, H. F.; De Almeida, W. B. *J. Phys. Chem. A* **2005**, *109*, 3209−3219.
(34) Miyake, K.; Yasuda, S.; Harada, A.; Sumaoka, J.; Komiyama, M.; Shigekawa, M. *J. Am. Chem. Soc.* **2003**, *125*, 5080−5085.

(35) Girardeau, T. E.; Zhao, T.; Leisen, J.; Beckham, H. W.; Bucknall, D. G. *Macromolecules* **2005**, *38*, 2261−2270.
(36) Isono, T.; Otsuka, I.; Kondo, Y.; Halila, S.; Fort, S.; Rochas, C.; Satoh, T.; Borsali, R.; Kakuchi, T. *Macromolecules* **2013**, *46*, 1461−1469.
(37) Kalyanasundaram, K.; Thomas, J. K. *J. Am. Chem. Soc.* **1977**, *99*, 2039−2044.
(38) Postmus, B. R.; Leermakers, F. A. M.; Cohen Stuart, M. A. *Langmuir* **2008**, *24*, 1930−1942.
(39) Litvinchuk, S.; Lu, Z.; Rigler, P.; Hirt, T. D.; Meier, W. *Pharm. Res.* **2009**, *26*, 1711−1718.